Professur für Hydrologie

der Albert-Ludwigs-Universität Freiburg i. Br

Moritz Mährlein

Streamflow response to forest fire and salvage harvesting in a snow dominated catchment: a model-based change detection approach

Supervisor: Prof. Dr. Markus Weiler (Albert-Ludwigs-Universität Freiburg)
Co-Supervisor: Prof Dr. Dan Moore (University of British Columbia)

Master Thesis

July 2016

Declaration of Authorship

I, Moritz Mährlein, hereby declare the originality of this thesis. I confirm that the presented work is my own, that all work of others is quoted properly and that I have acknowledged all main sources of my help.

Vancouver, 10th of July 2016

Abstract

Forest fires affect hydrology in number of ways ranging from making the soil hydrophobic to removing the canopy and thus raising energy inputs to a below-canopy surface. There is a range of approaches to study the impact of canopy removal on streamflow. In this study, a model based change detection approach was implemented in order to evaluate the impact of the McLure Forest Fire on the streamflow of Fishtrap Creek, which burned 60% of the catchment in the summer of 2003. Following the fire, the burned area was salvage logged. Apart from the change detection, a second aim was to evaluate the uncertainty linked to the change of forest cover through time. Six different land cover data sets representing forest cover for the whole pre-fire study period from 1970 to 2003 were used to calibrate an HBV-EC model family for Fishtrap Creek using two different calibration algorithms. By comparing resultant calibrated parameter sets, it was shown that the different calibration sets led to a substantial variability in parameters. This indicates that the specification of land cover can be a significant source of parameter uncertainty. The model with the best performance was then selected to be used in the change detection analysis. For this purpose, a regression model was fitted between observed and simulated discharge using only pre-fire data. With the help of this regression model post-fire streamflow was predicted in order to simulate a non disturbed runoff. By comparing the simulated and observed time series, an earlier onset of the melt seasons with no increase in peak flows was identified, with a higher consistency following the salvage logging. Two more regression models were set up in order to test the effect of the fire statistically. The "full" model accounted for the effect of the period (pre-fire and post-fire), the "reduced" model was based on the discharge values. When comparing them by an ANOVA, two main periods of change were identified: early winter linked to pre-harvest runoff events and early spring freshet linked to post-harvest events. Apart from these melt dominated seasons, no change in runoff was detected.

Zusammenfassung

Waldbrände beeinflussen die Hydrologie eines Einzugsgebietes in verschiedenster Weise, von der Hydrophobisierung der Böden bis hin zum Entfernen der Baumkrone, wodurch eine erhöhte Energiezufuhr in das System ermöglicht wird. Es existieren viele verschiedene Methoden, um die Auswirkungen von Waldbränden und Holzernte zu untersuchen. In dieser Masterarbeit wird ein modellbasiertes Verfahren angewendet um die Änderung im Abfluss nach einem Waldbrand zu evaluieren. Es werden die Auswirkungen des McLure Forest Fires auf das Einzugsgebiet des Fishtrap Creek untersucht, welches im Jahr 2003 zu 60% abbrannte. In den folgenden zwei Jahren wurde das Einzugsgebiet zusätzlich zu dem Waldbrand, durch das Abernten der verbrannten Flächen noch weiter beeinflusst. Neben dieser Evaluation wurde in der vorliegenden Arbeit die Auswirkung von veränderter Landnutzung während des Modellierungszeitraumes auf die Modellperformance untersucht. Hierfür wurden sechs verschiedene Landnutzungsdatensätze, die den gesamten Modellierungszeitraum von 1970 bis 2003 abdecken, genutzt um mithilfe zweier verschiedener Algorithmen eine HBV-EC basierte Modellfamilie zu kalibrieren. Im Vergleich der kalibrierten Parametersätze zeigte sich eine hohe Variabilität die mit den verschiedenen Landnutzungsdaten verknüpft werden kann und als bisher nicht untersuchte Ursache für Parameterunsicherheit interpretiert wurde. Um die Änderungen im Abfluss zu evaluieren, wurde das am besten kalibrierte Modell aus der Modellfamilie gewählt. Anhand dessen wurde ein Regressionsmodel zwischen den observierten und simulierten Daten auf den Zeitraum vor dem Waldbrand kalibriert. Mithilfe dieses Modells wurde für den Zeitraum nach dem Waldbrand Abfluss für ein ungestörtes Einzugsgebiet simuliert. Im Vergleich des simulierten Abflusses mit dem gemessenen Abfluss konnte eine vorzeitige schmelzwasserdominierte Hochwasserspitze ausgemacht werden. Eine Vergrößerung des maximalen Abflusses wurde nicht sichtbar. Dieser Effekt zeigte sich verstärkt nach dem die Waldbrandflächen abgeholzt wurden. Anhand zwei weiterer Regressionsmodelle wurde die Auswirkung des Waldbrandes statistisch überprüft. Eine ANOVA wurde zwischen den beiden Modellen durchgeführt, wobei ein Modell den Einfluss des Zeitraumes (vor dem Waldbrand im Vergleich zu nach dem Waldbrand) berücksichtigte, während das zweite lediglich den Zusammenhang zwischen Abflüssen berücksichtigt. Hier zeigte sich, dass besonders zwei Zeiträume beeinflusst wurden: im frühen Winter passend zu den erhöhten Abflüssen vor der Abholzung und der Zeitraum der vorzeitigen Schmelzwasserabflüsse im Frühling. Neben diesen beiden Perioden zeigte die statische Auswirkung keine weiteren beeinflussten Zeiträume.

Acknowledgements

First and foremost, I would like to thank my supervisor Prof. Dr. Markus Weiler for making this thesis possible. A special thanks goes to my co-supervisor Prof. Dr. Dan Moore for his support, enthusiasm and his answers to all my questions.

Furthermore, I would like to thank my friends and family for supporting me during the thesis, everyone doing their best to help me. I would especially like to thank my parents, without whose financial support and patience I would not have been able to do this thesis.

Contents

List of Figures

List of Tables

1 Introduction

Forests influence hydrology in a number of key ways. Forests generally have higher interception loss and transpiration compared to open sites with low vegetation (Rothacher, 1963; Hewlett, 1961). Through the effects of shading and sheltering from the wind, forests reduce energy inputs to a below-canopy snow surface and reduce melt rates (Winkler *et al.*, 2005). Forest soils, especially in temperate climatic zones, typically have sufficiently high infiltration capacities. This means that infiltration-excess overland flow rarely, if ever, occurs at undisturbed sites (Cheng, 1988; Wondzell & King, 2003).

Reduction or removal of forest canopies modifies processes such as interception loss and snow dynamics, which, in turn, modifies streamflow patterns (Winkler *et al.*, 2005; Dhakal & Sidle, 2004). In addition, forest disturbance, harvesting, and other related activities can modify runoff generation processes. For example, intense fires can make the soil hydrophobic and they increase the risk of infiltration-excess overland flow, at least for the first year or two following the fire. Letey (2001) concluded forest fires can make soil hydrophobic by producing volatile organic gases, which condense in cooler layers below the surface. Although it has been shown, that post wildfire response is linked to the varying alteration of the soil. Bento-Gonçalves *et al.* (2012) studied erosion following wildfires and found low erosion values within a year after the fire. They linked the low erosion to the duff coverage being only partially consumed while the remaining duff provided detention storage, therefore preventing surface flow.

Logging practices such as yarding with skidders can cause soil compaction, which enhances overland flow production (La Marche & Lettenmaier, 2001; Jones *et al.*, 2000) . Logging roads modify runoff generation in two ways: first, their surfaces tend to have low infiltration capacity and thus generate overland flow on a regular basis (Tague & Band, 2001) and, second, roads and their ditches tend to intercept subsurface stormflow, convert it to overland flow in the ditch or over the road surface (Sidle & Onda, 2004). Depending on the connectivity of the road and the drainage network to the channel network, road-related overland flow may be routed more rapidly to a channel, thus generating a flashier hydrograph response and higher peak flows (La Marche & Lettenmaier, 2001).

Decades of research has focused on the effects of forest disturbance and harvesting on streamflow, and has led to a number of generalizations. Disturbance and harvesting generally increase annual water yield and also increase late summer-autumn baseflow. Also, peak flows typically increase, although the magnitude, frequency and persistence of effects varies on both catchment characteristics and the spatial pattern of disturbance/harvesting intensity in the catchment.

In medium to large catchments (e.g., 10 to 100 km^2 and larger), forest cover conditions are rarely uniform. Instead, there is typically a mosaic of stands of different ages, species and tree densities that reflects the spatial and temporal patterns of disturbance and harvesting within a catchment. This shifting nature of forest cover within a catchment has implications for hydrologic modelling. Most hydrologic models treat land cover characteristics as static, despite the fact that they can change substantially over decadal time scales. When calibrating a model, using land cover information from one point in time may result in biased parameters. It may be that different parameter sets would result from using land cover determined at different times during the calibration period, introducing a source of parameter uncertainty on top of those associated with model structure and errors in input and streamflow data, which have been the focus of much research over the last two decades. Beven (1989) and Beven (1993) pointed out the importance of respecting the limitations of hydrological models and of keeping in mind model uncertainty, which is linked to the heterogeneous reality and input data.

In small headwater catchments (e.g., up to a few km^2 in area), paired-catchment studies have been successfully used to estimate the effects of forest cover changes on streamflow (Bates, 1921; Hewlett, 1982; Owens *et al.*, 2006). The paired catchment approach utilizes two catchments located near each other and being a similar in land use, climate, size and physiogeography (Hewlett, 1971). A statistical relationship is established between the catchment outlet responses before treatments are applied to one catchment. The control catchment remains undisturbed and is used to account for meteorological influences. When looking at larger catchments, finding a nearby catchment which would be sufficiently similar in characteristics such as hypsometry, soils, geology, vegetation and exposure to the same weather systems and then being able to use it as a control in a paired catchment study is rare. And it is even rarer to find a potentially useful control catchment that is gauged. Therefore, our understanding of the effects of forest cover changes on streamflow is not as developed as that for headwater catchments.

Recognizing these challenges to applying the paired-catchment approach to medium to large catchments, a number of researchers have advocated the use of simulation models. Some researchers have applied a process-based model using different forest cover scenarios (e.g., fully forested versus partially harvested) and then assumed that the difference between the simulations is a valid estimate of the effect of forest harvesting (Schnorbus & Alila, 2013). Seibert & McDonnell (2010) calibrated a hydrological model to different periods before and after a forest fire, and interpreted differences in the calibrated parameters in relation to hydrologic changes associated with the fire. Bowling *et al.* (2000) calibrated a model to a period with relatively slow forest cover change and then ran the model for the entire period using those calibrated parameters.

They then conducted a paired-catchment analysis by treating the simulated streamflows as a ”virtual control.” The analysis was conducted using streamflow measures at an annual time step, so temporal autocorrelation should not have been an issue. Zegre et al. (2010) used a model in a similar way but, owing to the short periods of record available, analyzed daily time series, for which temporal autocorrelation cannot be ignored. To address this problem, they applied generalized least squares regression, which can explicitly incorporate the effects of autocorrelation.

The objective of this research is two-fold. The first is to explore the magnitude of parameter uncertainty associated with uncertainty in or lack of accounting for forest cover changes through time. The second is to quantify the effects of a severe wildfire and follow-up salvage logging on streamflow in a snow-dominated catchment. To accomplish the second objective, a new variation on model-based change detection is developed and applied.

2 Method

2.1 Study site description

The study focused on Fishtrap Creek, which drains into the North Thompson River southwest of Barriére, British Columbia. Fishtrap Creek and its main tributary Skull Creek drain a rolling hill plateau in the headwaters with steep incised slopes along the lower reaches of both creeks. The catchment vegetation is dominated by the Montane Spruce biogeoclimatic zone. The hydrologic regime is snow-dominated, with the spring freshet typically beginning late March to mid-April and extending into June or July. Following the freshet, the hydrograph is dominated by a gradual recession from late summer to late winter, with occasional responses to late-summer or autumn rain events.

Water Survey of Canada has maintained a streamflow gauging station, "Fishtrap Creek near McLure", instrumented with a concrete v-notch weir. At the gauging station, the catchment area is 140 km^2. Elevation within the catchments ranges from 610 m at the weir to 1660 m (Figure 2.1).

In August 2003, the McLure Forest Fire burnt an area of over 260 km^2 southwest of the city of Barrière (Eaton *et al.*, 2010). It was classified as a Rank 6 fire, which is the highest and most hazardous category in the BC Wildfire Services Wildfire Rank. The fire spread over 62% of the area of the Fishtrap Creek Catchment, which was severely burned. The burned area includes the riparian zone along the lower reaches. Subsequent to the forest fire in 2003, salvage logging occurred on an area estimated as 20% of the catchment in 2004 to 2005 (Owens *et al.*, 2013).

2.2 Data

In this section basic information, gathering and preparation of data will be discussed.

2.2.1 Hydrometeorological Data

Daily streamflow data are available from September 1970 to present, and were downloaded from Environment Canada. Water Survey of Canada quality checks all streamflow data prior to publication. Missing values due to technical failure and ice conditions are estimated by interpolation, extrapolation, comparison with other streams or by correlation with meteorological data. Infilled data due to ice conditions are coded as "B";

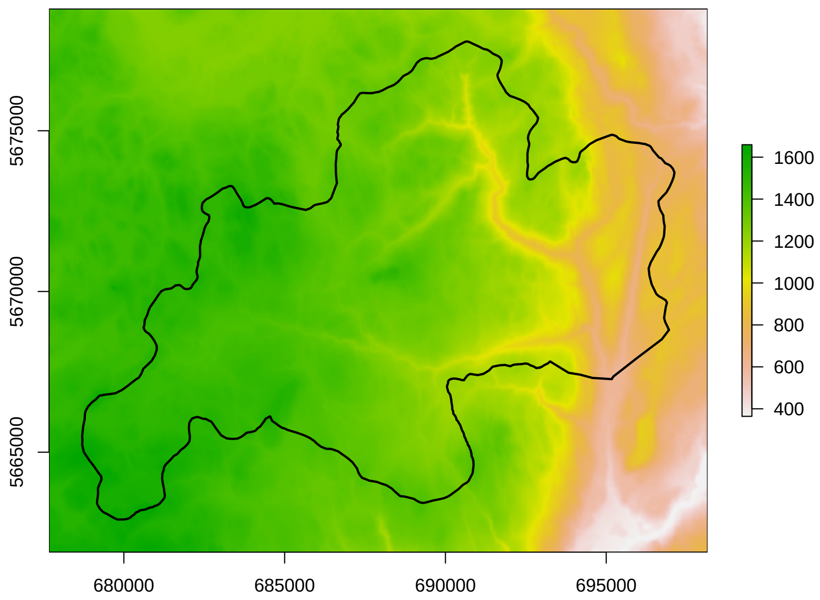

Figure 2.1: Digital Elevation Model of Fishtrap Creek Catchment with catchment outline

other estimated values are coded as "E." A total of 1591 missing values and 143 partially missing daily values were present in the streamflow record.

Table 2.1 summarizes the parameters measured and periods of records for weather stations located near Fishtrap Creek. The McLure station was chosen because of its proximity to the catchment and the relatively long record. To infill gaps in precipitation and temperature, data collected at the stations Barrière, Darfield and Kamloops Airport were used. All are located within the North Thompson River valley east and southeast of the catchment and are operated by Meteorological Service of Canada. For missing data at the McLure station, a regression model was used to predict precipitation and temperature at McLure station based on values at the other stations. Separate regression models were fit for each month.

Another input variable required for hydrological modelling is potential evapotranspiration data, which was calculated within the Raven hydrological framework, described in section 2.3. The evapotranspiration is calculated by using the empirical Hamon Equation Hamon (1961), which utilizes monthly mean and daily temperature as follows:

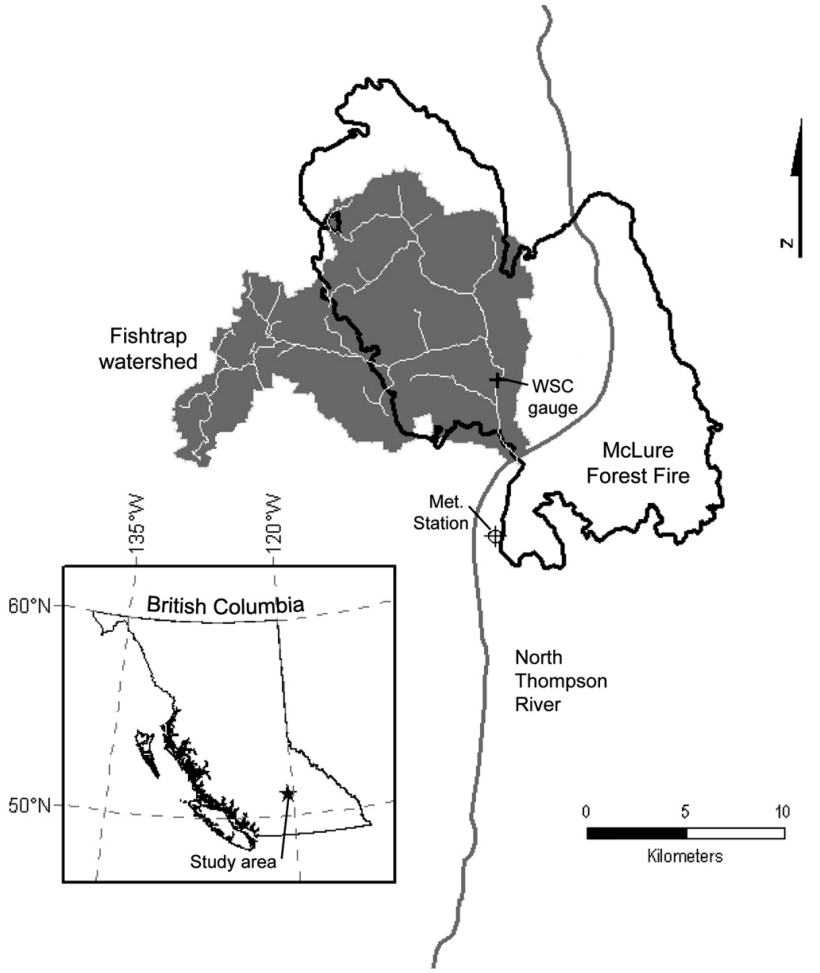

Figure 2.2: Extension of the McLure Forest Fire, altered from Owens *et al.* (2013)

$$PET = 1115 * \frac{e_{sat} * L_d^2}{T_{ave}} \tag{2.1}$$

where e_{sat} is the saturated vapor pressure [kPa], T_{ave} the daily temperature [K], L_d is the day length [d].

2.2.2 Spatial Data

To determine hydrological response units for modelling, elevation and land cover data are required. For elevation, the Canadian Digital Elevation Model was used. It can be downloaded from the Natural Resources Canadas Website. The catchment outline was derived from a shapefile provided by Water Survey of Canada.

Table 2.1: Hydrometeorological Data

Station	Climate-ID	Parameter	Range	Missing Values
McLure	1165030	Temperature	01.10.1983 - 29.11.2009	303
		Precipitation	01.04.1967 - 29.11.2009	303
Barrière	1160670	Temperature	12.11.1955 - 31.10.1996	1126
		Precipitation	12.11.1955 - 31.10.1996	1126
Darfield	1162265	Temperature	17.11.1962 - 13.11.2015	62
		Precipitation	01.04.1956 - 13.11.2015	62
Kamloops Airport	1163780	Temperature	01.01.1951 - 12.06.2013	0
		Precipitation	01.01.1951 - 12.06.2013	0

Land cover was represented as three different classes: forest, open and lake. Six aerial photograph data sets from 1974, 1981, 1986, 1990, 1995 and 2000 were used to map forest cover by M. Chuang (pers. comm.). Chuang distinguished three forest cover types: fresh clearcut, young forest and old forest. In this study, the young forest and old forest were grouped together.

Lakes were classified using shapefiles downloaded from the Atlas of Canada, an online data base for multiple spatial data by Natural Resources Canada. Remaining areas, not classified as forest or lake, were defined as open areas. By combining the three land cover types, an area-wide continuous shape file was created.

Hydrological response units (HRUs) for modelling were defined using the DEM and rasterized land-cover data. HRU classes are defined based on elevation band (in 100 m steps), slope and aspect (computed from the DEM) and the land cover classes. Aspect was categorized following three classes: less than 20°, between 20° and 45° and steeper than 45°. For the slope, HRUs were categorized as facing North (0° to 180°) or South (180° to 360°). A focal filter was used to lower the resolution in order to reduce the number of resulting HRU's to reduce computation times. Figure 2.3 shows the resulting HRU for 1974 land cover as an example.

2.3 Model

This study used an emulation of HBV-EC, which is Environment Canada's version of Hydrologiska Byråns Vattenbalansavdelning model (HBV) (Bergström *et al.*, 1995) and its structure is described in detail in Hamilton *et al.* (2000). It is a semi-distributed lumped parameter precipitation-runoff model. Required parameters are listed in Table 2.2.

The model operates on a daily time step. Precipitation and temperature are extrap-

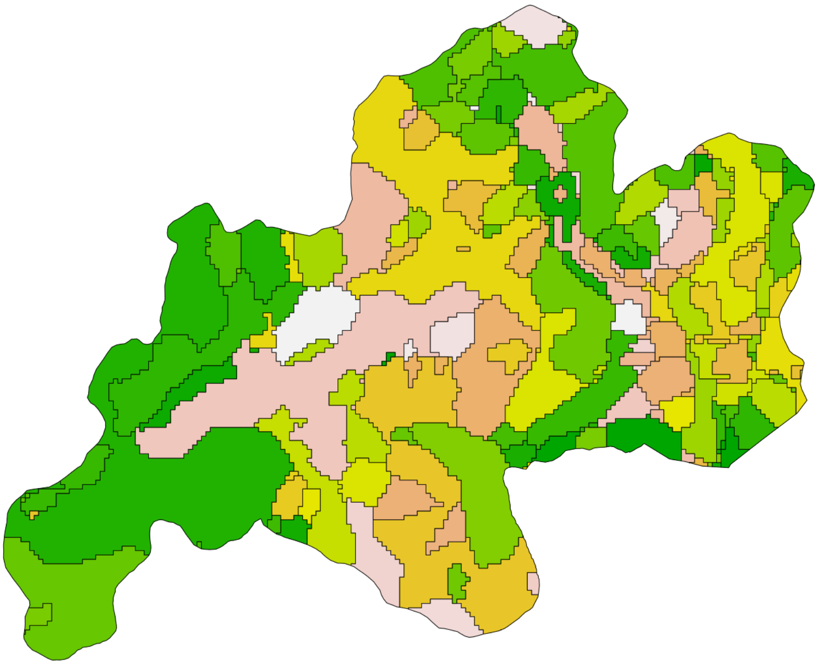

Figure 2.3: Hydrologic Response Units;Exemplary result from processing spatial data using 1974 land cover; Colors responding to a combined parameter value derived from

olated from the weather station to the center of each HRU to include lapse rate effects. The model accounts for interception loss from forest canopy, and simulates the accumulation and melt of snow, including calculation of snowpack cold content and water retention. Snow melt is computed using a temperature-index approach, with the melt factor allowed to vary as a function of time of year, land cover, and slope-aspect. Rain and/or meltwater are added to the soil moisture storage. The soil routine regulates drainage based on the ratio of soil moisture to field capacity, and evapotranspiration is a function potential evapotranspiration and the ratio of soil moisture to field capacity.

Drainage of water from the soil moisture storages for each HRU is routed through lumped reservoirs. In the configuration used here, the model features two parallel reservoirs. The fast reservoir, which can be nonlinear depending on the value of a coefficient, represents fast flow paths such as overland flow and shallow subsurface flow,

Table 2.2: Parameter used in the Raven Emulation of HBV-EC

Parameter	Description
RFCF	Rainfall correction factor
SFCF	Snowfall correction factor
TF_{rain}	Fraction of rainfall not lost ot interception
TF_{snow}	Fraction of snowfall not lost ot interception
T_{lapse}	Temperature lapse rate
TT	Threshold temperature limit for snow/rain [°C]
TT_i	Temperature interval for mixture of snow and rain [°C]
C_{min}	Minimum Melt factor [mm/°C/d]
C_{max}	Maximum Melt factor [mm/°C/d]
MRF	Ratio between the melt factor in forest to open areas
CRFR	Melt factor for freezing of liquid water in snow
WHC	Maximum liquid water content of snow
AM	Aspect melt factor
FC	Field capacity [mm]
L_p	Limit for potential evaporation
β	Exponent in soil drainage function
f	Fraction of catchment contributing to slow runoff
K_1	Outflow coefficient for fast reservoir
α	Exponent in outflow for fast reservoir
K_2	Outflow coefficient for slow reservoir

while the slow reservoir conceptually represents baseflow associated with discharge of deeper groundwater.

This study used an emulation of the HBV-EC model within the Raven modelling platform Craig & the Raven development team (2016). The Raven platform has a flexible structure that allows the user to build a model by choosing among a range of spatial structures and process representations. Within Raven, model equations are framed as differential equations that are solved using robust and fast numerical schemes.

2.4 Calibration and validation

In order to calibrate the model, two different approaches were used, Particle Swarm Optimization (PSO) and Dynamically Dimensioned Search (DDS).

Particle Swarm Optimization (Kennedy & Eberhart, 1995) is a population based optimisation algorithm, which does not utilize selection like evolutionary algorithms. It starts with a group of random parameters and searches optima by updating generations. It finds the best solution by adjusting the particles postion based on its own and its companions' position. The Dynamically Dimensioned Search Algorithm Tolson & Shoemaker (2007) is a search algorithm, which is designed for calibrations with many parameters. It was demonstrated to be more efficient and more robust than common evolutionary algorithms like SCE Duan *et al.* (1993) when using more than 10 parameters for watershed model calibration. DDS starts searching globally and then transitions into a more local search towards the iteration limit defined by the user, by dynamically reducing the number of dimensions in the neighborhood.

Both approaches were used to calibrate models using the six land cover data sets, resulting in a model family of 12 calibrated models. The Nash-Sutcliffe Efficiency (NSE, Nash & Sutcliffe (1970)) was used as an objective function for all calibrations. The calibration procedures were executed within the Ostrich (Matott (2005) platform, a multi algorithm and model independent optimization software application. To calibrate the set-up Raven HBV-EC model, parameter ranges for all parameters were defined. The objective function NSE was calculated by Raven and then evaluated by Ostrich to determine model fit and select parameters for the next model run.

The calibration/validation procedure was based on a split sample approach, in which the modelling period was split into a 2/3 calibration phase (1970 to 1992) and a 1/3 validation period (1992 to 2003).

2.5 Change detection

In the following section, the change detection approach is described. The method is loosely based on the method presented in Zégre *et al.* (2010). In broad terms, the approach involves calibrating a hydrological model to pre-disturbance data, then using the calibrated model to simulate streamflow for both the pre- and post-disturbance periods. The simulated streamflow is then treated as a ”virtual control” in a paired-catchment analysis.

As a first step, each year was split into consecutive 5-day periods, and the simulated and observed discharge series were averaged within each of the 73 5-day periods each year. Averaging the runoff into these ”pentads” smooths out timing differences between the simulated and observed runoff, while retaining sufficient resolution to detect changes in runoff timing of a week or more. Prior to the change detection analysis, discharge was log-transformed in order to satisfy the assumptions underlying linear regression, specifically linearity of the relation and homogeneity of variance. For each of the pentads, observed discharge was regressed against simulated discharge for the pre-fire period:

$$y_{pre} = b_0 + b_1 x_{pre} + e \tag{2.2}$$

where y_{pre} is the log-transformed observed discharge for the pre-fire period, x_{pre} is the log-transformed simulated discharge for the pre-fire period, b_0 and b_1 are coefficients estimated by ordinary least squares regression, and e is the residual.

The regression model was then used to generate a predicted time series of log-transformed discharge:

$$\hat{y} = b_0 + b_1 x \tag{2.3}$$

where x is the log-transformed simulated discharge (for both pre- and post-fire periods). The value of $\hat{y}$ represents, for the post-fire period, an estimate of what the log-transformed discharge would have been had the fire not occurred.

To test statistically for the effect of the fire, two regression models were fit between the observed log-transformed streamflow (y) and the log-transformed streamflow predicted by the regression model. The first is a reduced model, which is consistent with the null hypothesis that the fire and salvage logging did not influence streamflow:

$$\hat{y} = b_0 + b_1 \hat{y} \tag{2.4}$$

The second, called the ”full” model, includes a categorical variable to distinguish the pre-fire and post-fire periods. In terms of R syntax, the model can be expressed as follows:

$$\hat{y} \sim \hat{y} * period \tag{2.5}$$

where period is a categorical variable with two values, representing the two data periods, and the product ”$*$” indicates that all main effects of both variables and all their interactions are included. An analysis of variance (ANOVA) is conducted to compare the two models. If the p-value of the test is less than 0.05, then the full model explains significantly more variance than the reduced model, and the null hypothesis is rejected. The accepted hypothesis is that the fire and/or the salvage logging had a statistically significant influence on discharge for a given pentad.

Following the change detection, both time series were back-transformed to compare the discharge time series. To account for transformation bias, the discharge series were corrected following Baskerville (1972). Differences between predicted and observed post-fire discharge are then compared to assess the direction and magnitude of change in the streamflow regime after the forest fire.

3Results

3.1 Overview of the studyperiod

In this section, a brief overview of the study period is given. The data presented here was processed, as described in Section 2.2.

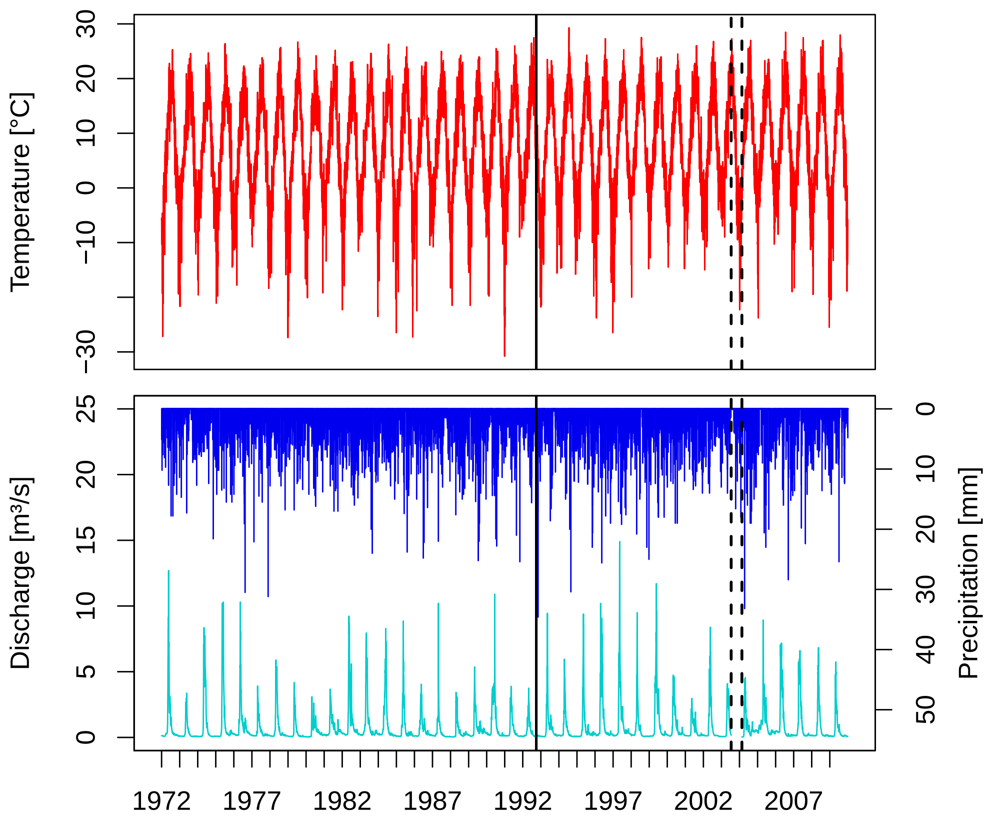

Figure 3.1: Timeseries of hydrometeorological data; the upper part of the figurepanel displays the daily temperature [$°C$], Precipitation [mm] as blue bars and Discharge [$m^3 s^{-1}$] as cyan line are shown in the lower part; the continuous vertical line marks the separation between calibration and validation while the dashed line shows the period of the forest fire.

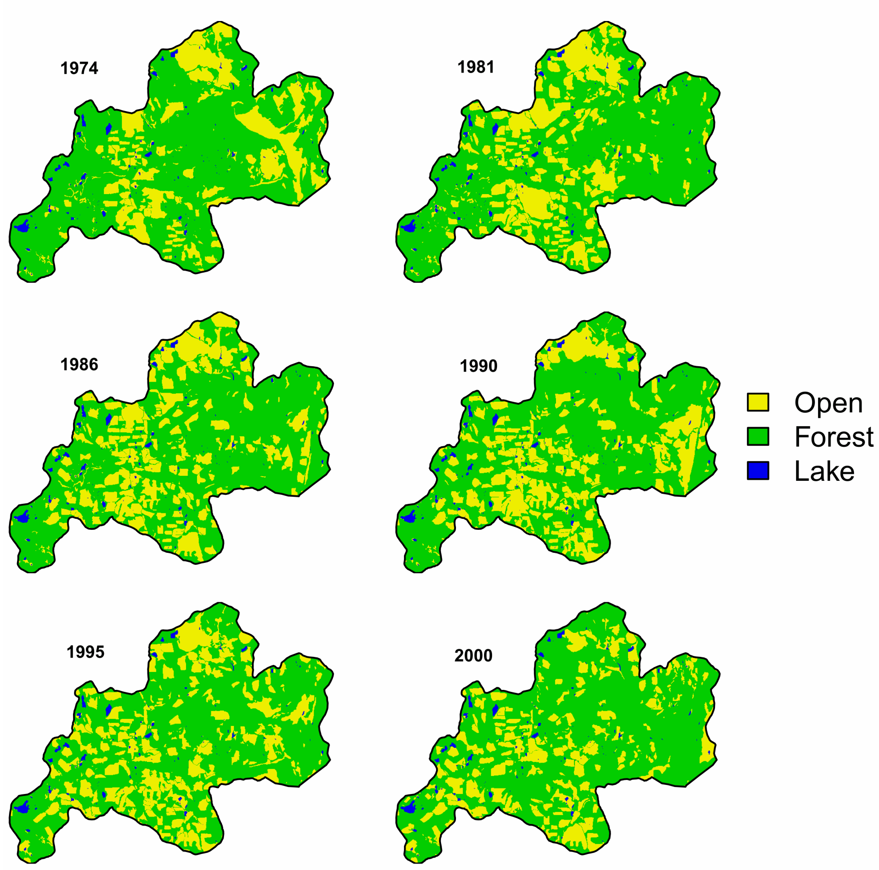

Figure 3.2: Landcover derived from the the six different datasets

Figure 3.1 presents time series of Hydrometeorological data used for the model calibration/testing and the change detection. The daily air temperature is illustrated in the upper part, precipitation and streamflow in the lower part. The spring snowmelt freshet is the dominant signal in the streamflow hydrograph, although there is substantial variability in the timing and magnitude.

Figure 3.2 shows the forest cover interpreted from the air photographs. It is clear that progressive forest harvesting and consequent regeneration produced substantial shifts in forest cover conditions over the study period which, in turn, had a clear effect on the HRUs (Figure 2.3).

3.2 Calibration and Testing

In the following section, results of the model calibration are displayed.

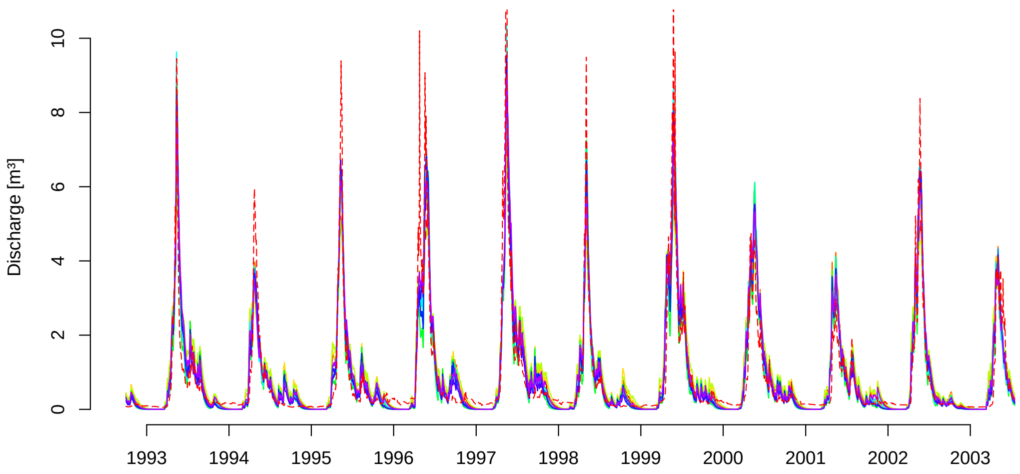

Figure 3.3: Hydrograph comparison for the validation period; Each colour indicates a different combination of optimization method and forest cover, and the dashed line is observed streamflow

Each of the 12 models resulting from the different calibration methods generated Nash-Sutcliffe efficiencies in the range 0.74 to 0.82 for calibration and 0.77 to 0.89 for validation (Table 3.1). Fig. 3.3 compares validation-period hydrographs of all calibrated models. The reduction to the calibration period is due to visual reasons. All model families generated similar hydrographs, with the greatest variability associated with autumn rain events. In general, most of these events were overpredicted, while a minority of the events were reproduced to a sufficient level, e.g. the autumn event in 2001 and 1995. All models matched the timing and shape of the freshet period hydrograph, but underestimated streamflow in winter. The freshet was underpredicted or matched for most of the years, and only in 2000 and 2001 did the majority of the models generate a peakflow higher than the observed. The underestimation of streamflow in winter is consistent throughout the calibration period for all models and streamflow is declining constantly from the last rain event in autumn until the first peak in spring caused by the freshet.

Table 3.1: NSE values for calibration and validation periods

Calibration	NSE_{cal}	NSE_{val}
DDS1974	0.75	0.81
DDS1981	0.78	0.85
DDS1986	0.76	0.82
DDS1990	0.74	0.77
DDS1995	0.79	0.86
DDS2000	0.78	0.87
PSO1974	0.81	0.88
PSO1981	0.8	0.87
PSO1986	0.81	0.88
PSO1990	0.8	0.86
PSO1995	0.82	0.89
PSO2000	0.79	0.85

Figure 3.4 illustrates the variability of each parameter as a function of land cover and calibration approach. To facilitate plotting on a single graph, the parameter estimates were normalized as follows:

$$P_i* = P_i/max(P_i) \tag{3.1}$$

where P_i represents the parameter estimate for a single combination of calibration method and forest cover. With this scaling, a clustering of points near 1 indicates little parameter variability, and an increasing range between 0 and 1 indicates higher variability.

The parameters that influence precipitation – including the rainfall and snowfall correction factors ($RFCF$ and $SFCF$) and the throughfall fractions (TF_{rain} and TF_{snow}) – exhibit relatively little variability. Most of the other parameters exhibit substantial variability, although it should be noted that the temperature thresholds for the rain-snow transition (TT) can take negative values, making the scaled values more difficult to interpret. Some parameters tend to separate into clusters (e.g. C_{min} and FC), while no calibration method leads to a values in between those clusters. But overall, there is no obvious separation based on the calibration method which would be either land cover or algorithm related, which suggests that most of the parameter variability is driven by the use of different forest covers to define HRUs.

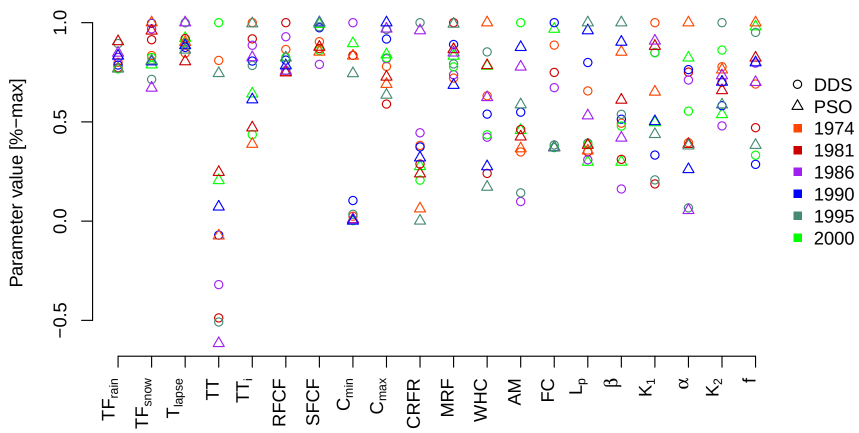

Figure 3.4: Comparison of parameter values generated by the different combinations of optimization method and forest cover

3.3 Change detection

Figure 3.5 displays a sample of scatterplots of observed versus modeled discharge, both in log-transformation. Each panel shows a pentad at the end of each month. The regression fit for the pre-fire period is shown as a solid line, while the dashed lines are the 95% prediction intervals. The pre-fire pentads, drawn as green dots, stay within the 95% prediction interval in the majority of the scatterplots, as expected. The few pre-fire predictions exceeding the 95% interval are outliers linked to high or low flows. To evaluate the impact of salvage logging, post-fire predictions were separated into pre-harvest and post-harvest predictions and drawn as yellow squares and red diamonds respectively. All of the four post-harvest predictions in April and two years of high flow in March show elevated values exceeding the 95% prediction and indicating an earlier snow melt dominated peakflow in spring. In contrast, the pre-harvest points tend to plot high from December to March, but follow the regression in spring and summer.

Figure 3.6 shows the results of the ANOVA change detection described in 2.5. The upper part of the figurepanel shows r^2 based on the pre-fire regression representing the model fit, the lower panel shows the p-values of the ANOVA, the main part of the change detection. The p-value drops below 0.05 for three periods, indicating a change in the runoff regime for these pentads. The first and third drop are persistent for multiple days and they both match the results of the scatterplots in Figure 3.5 for the pre-harvest and post-harvest early melt periods respectively. The findings are weakened

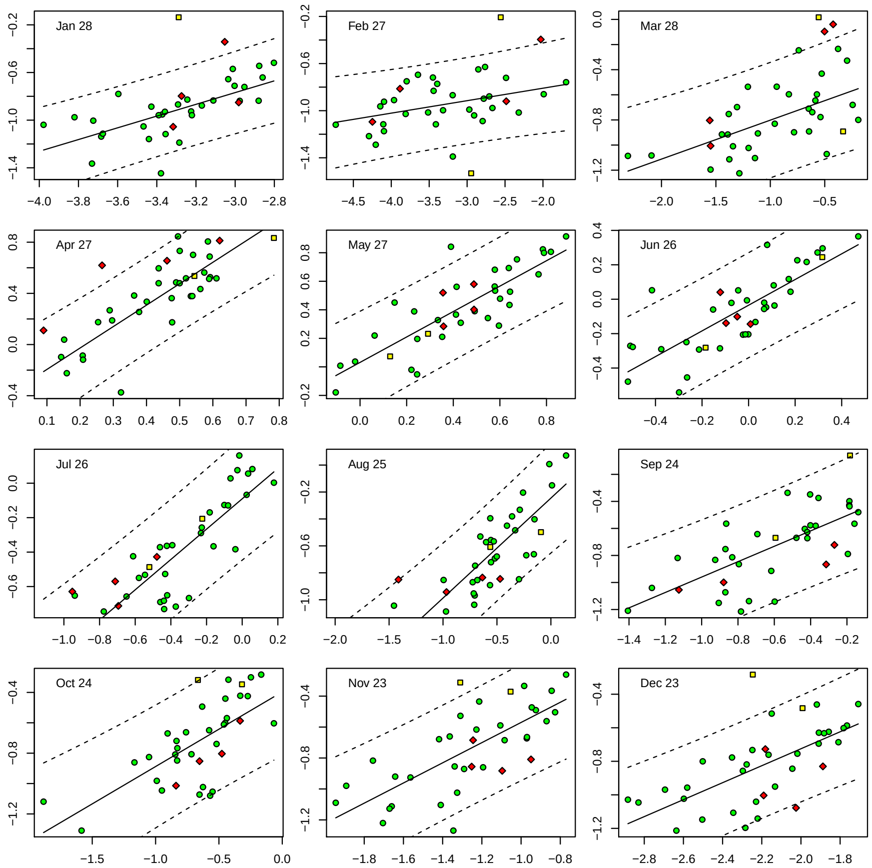

Figure 3.5: Sample of scatterplots of observed versus simulated discharge (both log-transformed) for 12 pentads distributed throughout the year. The date shown is the centre of the 5-day pentad. Green dots represent pre-fire data (1970-2003), yellow squares are post-fire and pre-logging (2004, 2005) and red diamonds are post-logging (2006-2009). The regression fit for the pre-fire period is shown as a solid line and the dashed lines are 95% prediction limits.

by the low r^2 in late February and late April, indicating a bad model fit during the early melt period.

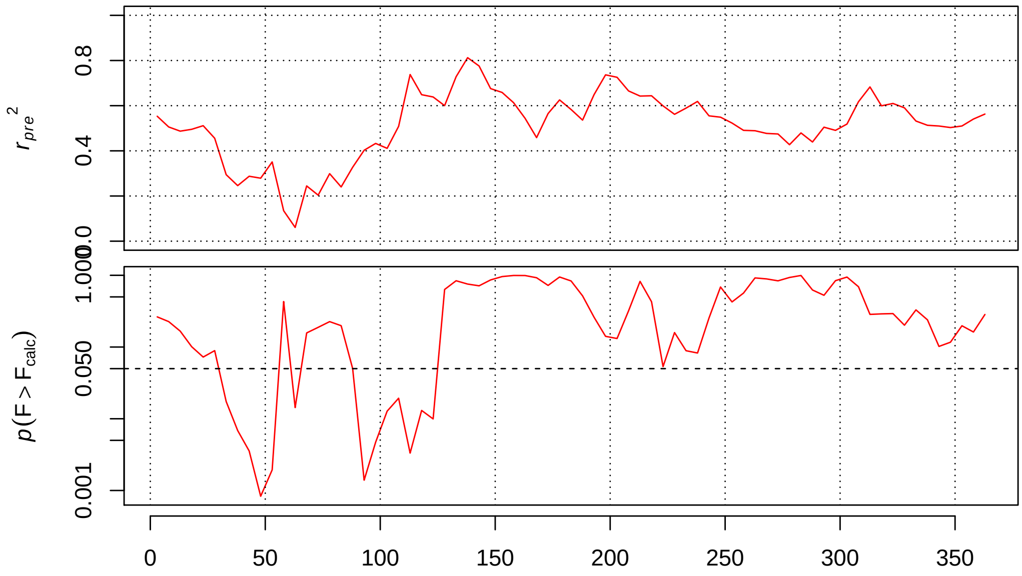

Figure 3.6: Results of the ANOVA change detection; the upper part of the figurepanel shows R^2 associated with the pre-fire regression; the lower part panel shows the p-value of for the ANOVA

Figure 3.7 displays the pre-fire predictions and observed streamflow in the upper and their difference in the lower panel. Both show the 95% prediction interval as a grey line. The upper panel suggests that the predicted streamflow follows the observed streamflow and matches its timing while the observed streamflow does not exceed the 95% prediction interval. The difference in models reveals the later prediction of peak flows in 1992 and 1997, while in other years peak flow is timed correctly but overpredicted (e.g. 1991,1993 and 2000). The difference does not exceed the 95% prediction interval.

Figure 3.8 presents the post-fire runoff, predicted streamflow and difference in the same way as the pre-fire discharge in Figure 3.7. The post-harvest discharge shows earlier peaks than the predicted runoff and an exceedance of 95% in 2006 and 2007. The difference shows that there is not only an earlier melt, but also a longer period of high flow. In the winter of 2004-2005 the observed runoff exceeded the prediction interval beginning in December 2004 and showing two minor peaks in early 2005, while the peak was overpredicted. In 2004 and 2008 relatively low peak flows occurred which did not exceed the prediction interval.

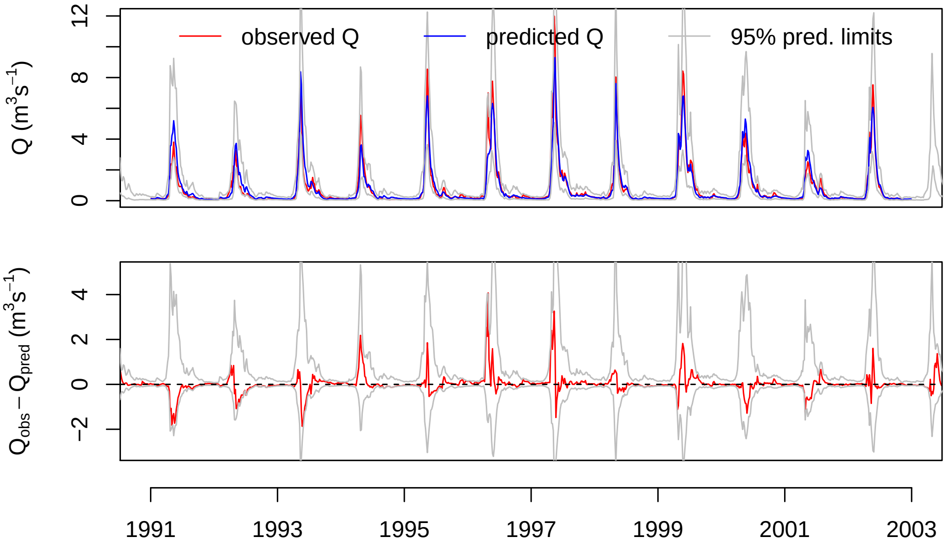

Figure 3.7: Predicted and observed streamflow in the pre-fire period, with 95% prediction limits.

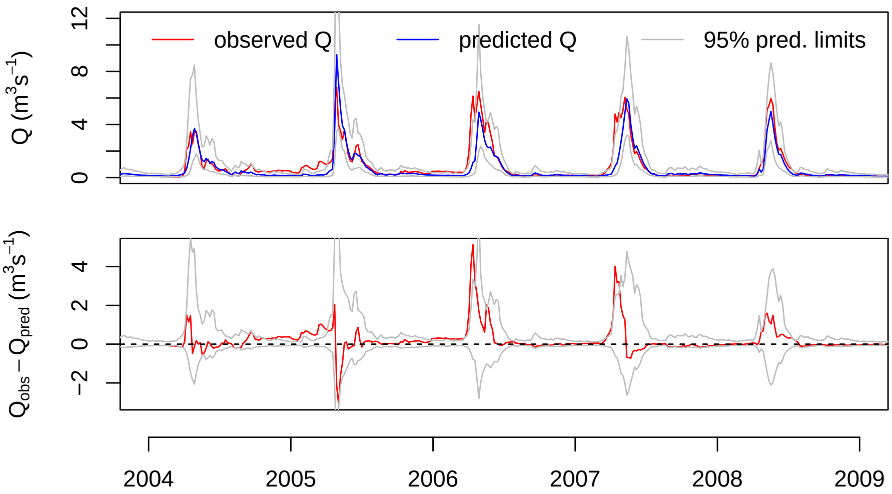

Figure 3.8: Predicted and observed streamflow in the post-fire period, with 95% prediction limits.

As seen in Figure 3.5, the post-fire data tend to plot higher than the pre-fire data in late winter and through April. This result is confirmed by the ANOVA (Figure 3.6), which indicates the effect of the fire was statistically significant for those periods at a 5% significance level. Consistent with these results, Figure 3.8 shows that, in many years, the spring freshet began earlier than predicted with predicted flow in April sometimes exceeding the 95% prediction limit. Of particular note is 2005, in which it appears that warm weather in late winter generated early rises in the hydrograph that are not apparent in the pre-fire period. By contrast, observed streamflow generally remained within the 95% prediction limits for the pre-fire period, with a less consistent occurrence of observed flow exceeding predicted on the rising limb of the freshet (Figure 3.8).

4 Discussion

This study demonstrated that many of the calibrated parameters in the HBV-EC model are sensitive to which land cover from within the calibration period was used to set up the model and define the HRUs. To the author's knowledge, this source of uncertainty has not been identified and quantified by previous research. Although time did not allow an assessment of other sources of uncertainty in this study, it would be valuable to extend the current study to quantify those other sources of uncertainty – model structure, input data, and streamflow data – to provide a more complete understanding of parameter uncertainty.

The finding that streamflow increases appeared to be confined to late winter and spring is broadly consistent with the results of Eaton *et al.* (2010), who used a purely statistical approach. They found an increase in annual runoff and a strong increase in April, but no apparent change in peak flow. Eaton *et al.* (2010) hypothesized that the fire and salvage harvesting desynchronized snowmelt runoff between disturbed and undisturbed portions, such that snow in disturbed areas began melting earlier, and made less of a contribution during May and early June, when most pre-fire peak flows occurred. The results of this thesis provide further support for this hypothesis by showing that, from May onward, there was no detectable increase in 5-day averaged streamflow. The change detection approach applied in this study was successful in detecting periods of increased streamflow in late winter and spring. However, the power of the test was likely limited by the relatively weak pre-harvest regressions, especially in winter, and it must be remembered that an inability to detect a change does not mean that a change did not occur. The lack of power was caused by an inability of the calibrated model to reproduce with high accuracy the interannual variations in streamflow. This was especially the case in winter, when r2 dropped to about 0.5.

The changes of streamflow within the pre-harvesting, which differ from the changes in the post-harvesting period might be linked to different reasons. The different findings of effects of forest fire on soil hydrophobicity (Letey, 2001; Bento-Gonçalves *et al.*, 2012) makes these changes hard to interpret. They can be also linked to the high temperature during the early winter of 2005.

Some of this uncertainty is likely associated with extrapolating precipitation data from a valley bottom location to the higher elevations on the plateau, which dominate the hydrology of Fishtrap Creek. However, some of the error is likely associated with model structure – in particular, inability to reproduce winter baseflow. It would be interesting to repeat this study using a different model, structured so as to reproduce winter baseflow more accurately. Another avenue for potentially improving the model would be to use additional information to assist in calibration. For example, the Ministry of Forests, Lands and Natural Resource Operations has monitored snowpack water equivalent at disturbed and undisturbed sites just outside the Fishtrap Creek catchment (Winkler *et al.*, 2005), and these could be used to help calibrate the parameters governing snow accumulation and ablation.

5 Conclusions

5.1 Summary of key findings

5.1.1 Calibration

The HBV-EC model calibration using the DDS and PSO optimization algorithms with six different land cover data sets resulted in a model family of 12 models. All of them produced discharge of a similar regime, with minor differences in total volume. Neither the land cover data set nor the calibration algorithm had a major effect on daily discharge simulations. All combinations of land cover and optimization algorithm tended to underestimate winter stream flows, likely because the model structure did not represent the aquifer structure correctly. All calibrations accurately reproduced the timing of the spring snow melt peak flow response, but underestimated the volume.

This analysis indicates that specification of land cover can be a significant source of parameter uncertainty, in addition to the effects of uncertainties in meterological and streamflow and model structure, which have been the subject of previous research (e.g.,Beven (1993); Beven & Freer (2001)).

5.1.2 Change detection

The change detection method applied in this thesis successfully detected change in the runoff regime of Fishtrap Creek after the McLure Forest Fire. The key changes included an earlier onset of the spring freshet in many years, and statistically significant higher streamflow between mid-March and early June. Streamflow changes were more consistent in the years following extensive salvage logging. The lack of a significant change in streamflow in late winter may reflect a lack of statistical power due to the weaker pre-fire regressions for that period.

The model-based change detection method developed and applied in this study is capable of detecting change in forest fire affected catchments, and shows promise as an effective tool for medium to large scale catchments for which effective control catchments are generally not available. The main challenge in applying the method is the need for long and complete records of air temperature and precipitation from a single weather station with a homogeneous record.

5.2 Recommendations for further research

The model-based change detection approach should be tested with different calibration methods to explore further the magnitude of this source of uncertainty. In addition, applying the approach with different model structures might improve its performance by allowing a better fit to the pre-disturbance streamflow data.

Another avenue for further research would be to use a process-based model to simulate directly the effects of the disturbance by modifying the land cover and HRUs to represent disturbed conditions. It would be interesting to compare simulations for a disturbed land-cover scenario to those for a control scenario, with pre-disturbance land cover to assess whether the model can reproduce the observed post-disturbance streamflow.

Bibliography

Baskerville, GL. 1972. Use of logarithmic regression in the estimation of plant biomass. *Canadian Journal of Forest Research*, **2**(1), 49–53.

Bates, Carlos G. 1921. First results in the streamflow experiment, Wagon Wheel Gap, Colorado. *Journal of Forestry*, **19**(4), 402–408.

Bento-Gonçalves, António, Vieira, António, Úbeda, Xavier, & Martin, Deborah. 2012. Fire and soils: key concepts and recent advances. *Geoderma*, **191**, 3–13.

Bergström, Sten, Singh, VP, *et al.* 1995. The HBV model. *Computer models of watershed hydrology.*, 443–476.

Beven, Keith. 1989. Changing ideas in hydrology - the case of physically-based models. *Journal of hydrology*, **105**(1-2), 157–172.

Beven, Keith. 1993. Prophecy, reality and uncertainty in distributed hydrological modelling. *Advances in water resources*, **16**(1), 41–51.

Beven, Keith, & Freer, Jim. 2001. Equifinality, data assimilation, and uncertainty estimation in mechanistic modelling of complex environmental systems using the GLUE methodology. *Journal of hydrology*, **249**(1), 11–29.

Bowling, Laura C, Storck, Pascal, & Lettenmaier, Dennis P. 2000. Hydrologic effects of logging in western Washington, United States. *Water Resources Research*, **36**(11), 3223–3240.

Cheng, JD. 1988. Subsurface stormflows in the highly permeable forested watersheds of southwestern British Columbia. *Journal of Contaminant Hydrology*, **3**(2), 171–191.

Craig, J.R., & the Raven development team. 2016. *Raven: User's and Developer's Manual v2.6.*

Dhakal, Amod S, & Sidle, Roy C. 2004. Pore water pressure assessment in a forest watershed: Simulations and distributed field measurements related to forest practices. *Water Resources Research*, **40**(2).

Duan, QY, Gupta, Vijai K, & Sorooshian, Soroosh. 1993. Shuffled complex evolution approach for effective and efficient global minimization. *Journal of optimization theory and applications*, **76**(3), 501–521.

Eaton, B.C., Moore, R.D., & Giles, T.R. 2010. Forest fire, bank strength and channel instability: the ‘unusual’ response of Fishtrap Creek, British Columbia. *Earth Surf. Process. Landforms*, **35**(10), 1167–1183.

Hamilton, A. S., Hutchinson, D. G., & Moore, R. D. 2000. Estimating Winter Streamflow Using Conceptual Streamflow Model. *J. Cold Reg. Eng.*, **14**(4), 158–175.

Hamon, W.R. 1961. Estimating Potential Evapotranspiration. *Journal of the Hydraulics Division,ASCE*, **87**, 107–120.

Hewlett, John D. 1961. *Soil moisture as a source of base flow from steep mountain watersheds*. Southeastern Forest Experiment Station, US Department of Agriculture, Forest Service.

Hewlett, John D. 1971. Comments on the Catchment Experiment to determine vegetal effects on water yield. *Water Resources Bulletin*, **7**(2), 376–381.

Hewlett, John D. 1982. Forests and floods in the light of recent investigation. *In: Proceedings of the Canadian Hydrology Symposium*.

Jones, Julia A, Swanson, Frederick J, Wemple, Beverley C, & Snyder, Kai U. 2000. Effects of roads on hydrology, geomorphology, and disturbance patches in stream networks. *Conservation Biology*, **14**(1), 76–85.

Kennedy, James, & Eberhart, Russell. 1995. Particle Swarm Optimization. *Proceedings of IEEE International Conference on Neural Networks*, 1942–1948.

La Marche, Jonathan L, & Lettenmaier, Dennis P. 2001. Effects of forest roads on flood flows in the Deschutes River, Washington. *Earth Surface Processes and Landforms*, **26**(2), 115–134.

Letey, J. 2001. Causes and consequences of fire-induced soil water repellency. *Hydrological Processes*, **15**(15), 2867–2875.

Matott, LS. 2005. Ostrich: An optimization software tool, documentation and user’s guide, Version 1.6. *University at Buffalo, Department of Civil, Structural, and Environmental Engineering*.

Nash, J.E., & Sutcliffe, J.V. 1970. River flow forecasting through conceptual models part I — A discussion of principles. *Journal of Hydrology*, **10**(3), 282 – 290.

Owens, Philip N., Blake, William H., & Petticrew, Ellen L. 2006. Changes in Sediment Sources following Wildfire in Mountainous Terrain: A Paired–Catchment Approach, British Columbia, Canada. *Water, Air, & Soil Pollution: Focus*, **6**(5), 637–645.

Owens, P.N., Giles, T.R., Petticrew, E.L., Leggat, M.S., Moore, R.D., & Eaton, B.C. 2013. Muted responses of streamflow and suspended sediment flux in a wildfire-affected watershed. *Geomorphology*, **202**(nov), 128–139.

Rothacher, Jack. 1963. Net precipitation under a Douglas-fir forest. *Forest Science*, **9**(4), 423–429.

Schnorbus, Markus, & Alila, Younes. 2013. Peak flow regime changes following forest harvesting in a snow-dominated basin: Effects of harvest area, elevation, and channel connectivity. *Water Resources Research*, **49**(1), 517–535.

Seibert, Jan, & McDonnell, Jeffrey J. 2010. Land-cover impacts on streamflow: a change-detection modelling approach that incorporates parameter uncertainty. *Hydrological Sciences Journal*, **55**(3), 316–332.

Sidle, Roy C, & Onda, Yuichi. 2004. Hydrogeomorphology: overview of an emerging science. *Hydrological Processes*, **18**(4), 597–602.

Tague, Christina, & Band, Larry. 2001. Simulating the impact of road construction and forest harvesting on hydrologic response. *Earth Surface Processes and Landforms*, **26**(2), 135–151.

Tolson, Bryan A, & Shoemaker, Christine A. 2007. Dynamically dimensioned search algorithm for computationally efficient watershed model calibration. *Water Resources Research*, **43**(1).

Winkler, RD, Spittlehouse, DL, & Golding, DL. 2005. Measured differences in snow accumulation and melt among clearcut, juvenile, and mature forests in southern British Columbia. *Hydrological Processes*, **19**(1), 51–62.

Wondzell, Steven M., & King, John G. 2003. Postfire erosional processes in the Pacific Northwest and Rocky Mountain regions. *Forest Ecology and Management*, **178**(1-2), 75–87.

Zégre, Nicolas, Skaugset, Arne E., Som, Nicholas A., McDonnell, Jeffrey J., & Ganio, Lisa M. 2010. In lieu of the paired catchment approach: Hydrologic model change detection at the catchment scale. *Water Resources Research*, **46**(11), n/a–n/a.